J Appl Electrochem (2009) 39:123–134
DOI 10.1007/s10800-008-9644-x

ORIGINAL PAPER

Preparation of Pt–Co alloy catalysts by electrodeposition for oxygen reduction in PEMFC

Yupa Saejeng · Nisit Tantavichet

Received: 2 April 2008 / Accepted: 23 July 2008 / Published online: 27 August 2008

Abstract Direct current (DC) and pulse current (PC) electrodeposition of Pt–Co alloy onto pretreated electrodes has been conducted to fabricate catalyst electrodes for oxygen reduction reaction (ORR) in proton exchange membrane fuel cells (PEMFC). The effect of plating mode and pulse plating parameters on the Pt–Co alloy catalyst structure, composition and electroactivity for the ORR in PEMFC has been investigated. The electrodeposited Pt–Co alloy catalyst indicates higher electrocatalytic activity towards the ORR than the electrodeposited Pt catalyst. The activity of the electrodeposited Pt–Co catalysts is further improved by applying the current in a pulse waveform pattern. The electrodeposition mode and the pulse plating parameters do not have the significant effect on the Pt:Co composition of deposited catalysts, but show the substantial effect on the deposit structures produced. The Pt–Co catalysts prepared by PC electrodeposition have finer structures and contain smaller Pt–Co catalyst particles compared to that produced by DC electrodeposition. By varying the Pt concentration in deposition solution, the Pt:Co composition of the electrodeposited catalyst that exhibits the highest activity is found. The Pt–Co alloy catalyst with the Pt:Co composition of 82:18 obtained at the charge density of 2 C cm^{-2}, the pulse current density of 200 mA cm^{-2}, 5% duty cycle and 1 Hz was found to yield the best electrocatalytic activity towards the ORR in PEMFC.

Keywords Electrodeposition · PEMFC · ORR · Platinum-cobalt catalyst · Pulse current

Y. Saejeng · N. Tantavichet (✉)
Department of Chemical Technology, Faculty of Science, Chulalongkorn University, Bangkok 10330, Thailand
e-mail: Nisit.T@chula.ac.th

1 Introduction

Fuel cells have caught a global attention in recent decades due to their high efficiency and environmental compatibility. Among various types of fuel cells, proton exchange membrane fuel cells (PEMFC) have shown a great promise as an alternative power generation for transportation applications due to their low operating temperature, fast start-up, high power density, and low emission of pollutants. However, some technical and economical challenges, such as the poor kinetics of the cathodic reaction, complicated catalyst loading process and the high cost of electrocatalysts, have to be overcome in order to make PEMFC commercially viable. It is well-known that the performance of PEMFC is hindered by the slow reaction of the oxygen reduction reaction (ORR) on the cathodic side of PEMFC [1]. One way to improve the cathodic performance is to develop more active catalysts used for the ORR. Alloying Pt with other metals such as Co, Ni and Fe has shown a good potential as an alternative approach to develop catalysts for the oxygen reduction kinetics [2–11] due to higher catalytic activity for the ORR compared to pure Pt. Among different Pt-based alloy catalysts used for the ORR, Pt–Co alloy catalyst has shown a great promise and has been the most studied Pt-based alloy catalyst [10, 12–17] since it has higher electrocatalytic activity towards the ORR than other Pt-based alloys [7, 8, 18, 19]. Moreover, the Pt–Co alloy catalyst was reported to have the better durability in an operating fuel cell environment than Pt catalyst [20].

There are various techniques for preparation of catalyst layers on carbon electrodes for membrane electrode assemblies (MEA) used in PEMFC, such as painting and spraying techniques. Normally, to prepare the Pt-alloy catalyst layers for PEMFC a multi-step-high-temperature

process is used [14, 20]. First, the Pt supported on carbon is prepared. It is followed by implagnation of the second metal on Pt supported on carbon. Then, alloying process is conducted at high temperature under controlled environment [10, 18, 21]. On the other hand, electrodeposition technique can prepare the alloy catalyst layer directly on the substrate in a single step which is relatively easy and more cost effective. Moreover, electrodeposition technique can produce uniform metal particle sizes and uniform metal distribution over the substrate with high selectivity from very small to large areas [22–24]. It has various operating parameters to control the amount of deposited metal, desired metal particle sizes, the desired metal structures and the desired compositions of the metal alloy. Although electrodeposition appears to be an attractive technique to prepare the catalyst layers for PEMFC, only a few works have studied the preparation of the catalyst layer for PEMFC by electrodeposition [23, 25–27], and most of them limit to Pt catalyst preparation. To our knowledge, no work has reported the preparation of Pt–Co alloy electrodes by electrodeposition for the ORR in PEMFC.

The purpose of this work is to show that the Pt–Co alloy catalyst electrodes can be prepared by electrodeposition and can be used effectively in the ORR in PEMFC. The Pt–Co alloy catalyst layer was prepared on pretreated carbon cloth using direct current (DC) and pulse current (PC) electrodeposition at the room temperature and was used on a cathode for the MEA fabrication to study the electroactivity towards the ORR. The suitable deposition conditions for the preparation of the Pt–Co catalyst layer were obtained through the study of DC electrodeposition and then were extended to study the preparation of the Pt–Co catalyst layer by pulse current electrodeposition. The morphological and structural characteristics and compositions of the electrodeposited catalyst layers were studied by SEM, EDX, TEM, and XRD.

2 Experimental

The preparation of the catalyst electrode by electrodeposition consisted of two steps. The first step was to prepare the non-catalyst electrode, the second was the electrodeposition of the catalyst on the carbon electrode. The non-catalyst layer consists of two sub-layers—hydrophobic layer and hydrophilic layer—formed on the carbon electrode. To prepare the non-catalyst electrode, first a carbon black (Vulcan XC-72) was treated at 300 °C for 3 h to remove the organic matter. Then, a carbon black was mixed with PTFE (60 wt.%) (Aldrich) and isopropanol (Fluka) in the ultrasonic mixer for 30 min. This mixture was painted on the carbon cloth (E-TEK) and dried at 300 °C for 2 h to form the hydrophobic layer. The next sub-layer (hydrophilic layer) was prepared by painting the mixture of PTFE, isopropanol and a carbon black with the addition of glycerol on top of the hydrophobic layer. The sub-layers were prepared in a way to have the total carbon black loading of 1.9 mg cm^{-2}. Then, the prepared non-catalyst electrode was dried at 300 °C for 2 h.

In the second step, the electrodeposition of catalyst layer on the pretreated electrode was conducted in a plating bath containing a solution of $H_2PtCl_6 \cdot 6H_2O$ and $CoSO_4 \cdot 7H_2O$ in 0.5 M H_2SO_4 to apply the catalyst layer on the electrode. Unless stated otherwise, the concentrations of $H_2PtCl_6 \cdot 6H_2O$ and $CoSO_4 \cdot 7H_2O$ used were 0.02 M and 0.1 M, respectively. The pretreated electrode was cut to a proper size and was placed in an electrode holder having an exposed area of 5 cm^2 for the electrodeposition. The titanium gauze was used as a counter electrode. An Autolab PGSTAT 10 potentiostat (Eco Chemie) was used to perform both DC and pulse current electrodeposition. During the electrodeposition the plating solution was stirred by magnetic stirrer at 300 rpm. After the electrodeposition, the electrode was dried at 80 °C for 2 h. The amounts of Pt and Co electrodeposited on the electrode were estimated from EDX technique based on the total amount of the catalyst electrodeposited on the electrode that was estimated from the weight difference before and after the electrodeposition.

The catalyst layers prepared by electrodeposition were characterized by SEM, EDX, XRD and TEM. The surface morphologies and compositions of the prepared catalysts were characterized using a scanning electron microscope (SEM) with the energy-dispersive spectroscopic (EDX) analyzer (JEOL JSM-6400). The structural characterizations were carried out with X-ray diffraction (XRD, Bruker AXS model D8 Discover). XRD provides the information of the lattice parameter (a_{fcc}) and the Pt–Pt mean atomic distance of catalyst based on the value of the maximum angle (θ_{max}) and the full-width at half-maximum ($B_{2\theta}$) of the peak. Scherer's equation [16, 28] was used to calculate the average particle size of the prepared catalyst based on broadening of the diffraction peak. Transmission electron microscopy (TEM, JEOL JEM-2100) was used to determine the particle sizes of the Pt–Co catalysts and to compare to those estimated by XRD.

To test the performance of the prepared catalyst for the ORR, the Pt–Co catalyst prepared by the electrodeposition was used as a cathode whereas a commercial E-TEK carbon paper electrode (10 wt.% Pt/C, 0.5 mg cm^{-2}) was used as an anode to fabricate the MEA. Both electrodeposited catalyst electrode and commercial electrode were painted with 5 wt.% Nafion solution (Fluka) to get the Nafion loading of 0.8 mg cm^{-2} on each electrode. Then, Nafion-impregnated electrodes and Nafion membrane were hot pressed at 137 °C for 2.5 min with a pressure of 65 kg cm^{-2} to form the MEA

for the fuel cell. The fabricated MEA was placed in a 5 cm^2 single cell fuel cell (Electrochem, Inc.) for performance test. The cell operation was carried out at 60 °C under ambient pressure and the performance test was conducted by the Autolab PGSTAT 10 potentiostat with the current booster (Eco Chemie). Hydrogen (99.999%, Praxair) and oxygen (99.999%, Praxair) were fed at anode and cathode, respectively, both at the flow rates of 100 $cm^3\ s^{-1}$ and 100% relative humidity.

3 Results and discussion

3.1 Pt–Co catalyst electrodes prepared by direct current (DC) electrodeposition

Table 1 shows the conditions for DC electrodeposition used in this study. The table also includes the total catalyst loadings and the compositions of Pt–Co catalysts obtained under those DC electrodeposition conditions. Two important parameters that control the properties of the electrodeposited metals—the charge density and the current density—are investigated. As expected, the higher charge density (i.e., 4 C cm^{-2}) leads to higher amount of catalyst loading. At the same applied charge density, the amount of catalyst loading obtained at the lower current density tends to be higher than that obtained at the higher current density since the electrodeposition of Pt at high current densities leads to intense hydrogen evolution and low current efficiency [29, 30], especially at closer to the mass transport control conditions. On the other hand, although in many cases the applied current density may affect the composition of the metal alloy [31], it is observed that the applied current density has only slight influence on the Pt–Co alloy composition of the catalysts where the Pt:Co ratios were found to be between 80:20 and 88:12.

Figure 1 shows the polarization curves of the PEMFC prepared by DC electrodeposition under the conditions shown in Table 1. Since the Pt–Co alloy composition of the catalysts is relatively unaffected by the applied current density and charge density, the influence of those electrodeposition parameters on the fuel cell performance should

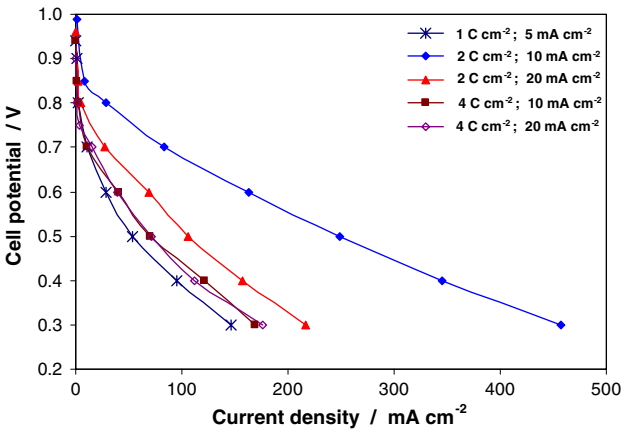

Fig. 1 Polarization curves of H_2/O_2 PEMFC with the Pt–Co catalyst electrodes prepared by DC electrodeposition

be due to the structure change of the Pt–Co catalysts. The electrode prepared at the charge density of 1 C cm^{-2} shows the lowest performance since it has the lowest amount of catalyst. Moreover, the SEM image shown in Fig. 2a reveals that the applied charge density of 1 C cm^{-2} is too low to allow the Pt–Co catalyst to cover the entire electrode surface. Thus, the active area of the catalyst is expected to be lower compared to those obtained at the higher charge densities. When the applied charge density is increased to 2 C cm^{-2} and higher (Fig. 2b, c), most part of the electrode is covered with Pt–Co catalyst. However, if the applied charge density is too high (i.e., 4 C cm^{-2}), the performance of the Pt–Co catalyst tends to decrease. This implies that after the entire surface is covered by the catalyst and the electrodeposition proceeds further, the existing crystals will grow to the bigger-grained catalysts leading to the lower active surface area. In addition, if too much amount of catalyst is loaded on the electrode, the catalyst particles will block each other resulting in the decrease in accessibility of reactant gas to catalyst sites and, consequently, the low catalyst utilization. As a result, the performances of the Pt–Co catalysts prepared at the charge current density of 4 C cm^{-2} are lower than those prepared at the charge current density of 2 C cm^{-2} (Fig. 1), although their Pt–Co catalyst loadings are substantially higher.

Table 1 Pt:Co composition and catalyst loading of the Pt–Co catalyst electrodes prepared by DC electrodeposition under different conditions

DC electrodeposition conditions		Pt:Co alloy compositions/ atomic ratio	Loading		
Charge (C cm^{-2})	Current (mA cm^{-2})		Pt (mg cm^{-2})	Co (mg cm^{-2})	Total (mg cm^{-2})
1	5	90:10	0.4180	0.0140	0.4320
2	10	88:12	0.6633	0.0274	0.6907
2	20	82:18	0.5571	0.0369	0.5940
4	10	80:20	1.2933	0.0977	1.3910
4	20	88:12	0.9201	0.0379	0.9580

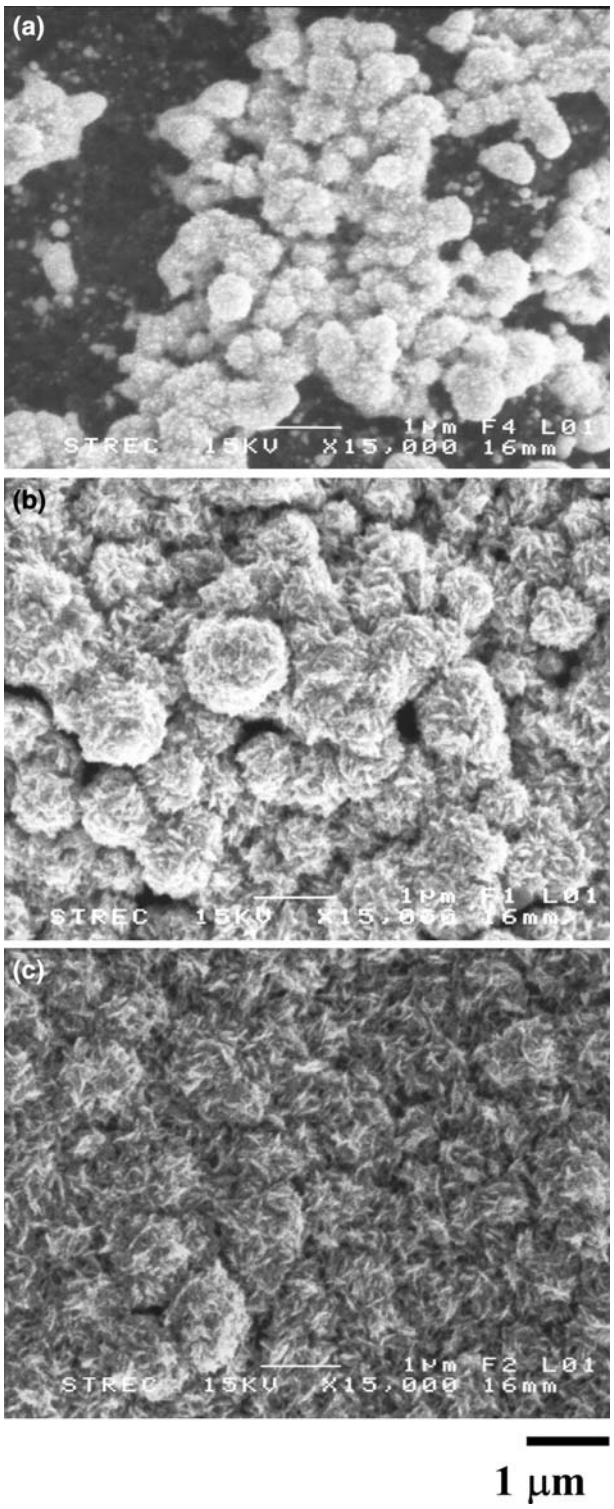

Fig. 2 SEM images of the Pt–Co catalyst electrodes prepared by DC electrodeposition at different charge densities and current densities. (**a**) 1 C cm^{-2} and 5 mA cm^{-2}; (**b**) 2 C cm^{-2} and 10 mA cm^{-2}; (**c**) 4 C cm^{-2} and 10 mA cm^{-2}

Compare the performance of the electrodes obtained at the same charge densities, the electrodes obtained at the current density of 10 mA cm^{-2} have higher performance than those obtained at the current density of 20 mA cm^{-2}. Normally, high applied current density enhances the nucleation rate of electrodeposition resulting in small-grained particles and fine crystal structure [32, 33]. However, if the applied current density is too high, big and coarse metal particles are produced [34] since the electrodeposition proceeds under (or closer to) the mass transfer control. This implies that the applied current density of 20 mA cm^{-2} may be so high that the electrodeposition may take place closer to the mass transfer conditions which leads to the formation of electrodeposit with big-grained and coarse structure. From Fig. 1, it is clearly seen that the Pt–Co catalyst electrode prepared at the charge density of 2 C cm^{-2} and the current density of 10 mA cm^{-2} has the highest performance in fuel cell testing. Then, it was chosen for further investigation using XRD for catalyst characterization analysis and EDX for compositional analysis.

The alloy formation of the Pt–Co catalyst can be confirmed by XRD spectra in Fig. 3. For a comparison, the Pt catalyst electrode prepared at the same conditions, but in a solution containing 0.5 M H_2SO_4 and 0.02 M $H_2PtCl_6 \cdot 6H_2O$, is also included (Fig. 3a). XRD spectra clearly show that the main characteristic peaks of the face-center cubic structure of crystalline Pt–Pt(111), Pt(200), Pt(220), Pt(311) and Pt(222)—shift to the higher 2θ values in the Pt–Co electrodeposited catalyst (Fig. 3b) compared to those in the Pt electrodeposited catalyst (Fig. 3a). The shifts to the higher 2θ values in the Pt–Co electrodeposited catalyst indicate alloy formation between Pt and Co due to a lowered lattice parameter of Pt on Pt–Co catalyst as a result of the incorporation of Co into the fcc structure of Pt [17–19, 35] during Pt–Co electrodeposition. The XRD patterns indicate that no evidence of metallic Co (i.e., reflection of Co(111) is expected to occur at $2\theta = 44.8°$) or Co oxides is found, which implies Co is incorporated into

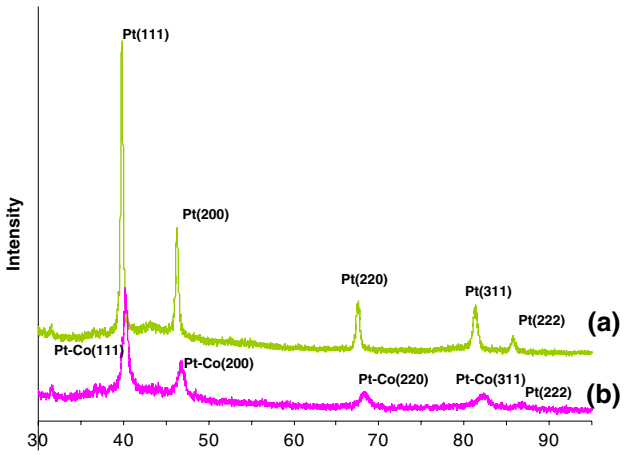

Fig. 3 X-ray diffraction patterns of the (**a**) Pt and (**b**) Pt–Co catalysts prepared by DC electrodeposition at 2 C cm^{-2} and 10 mA cm^{-2}

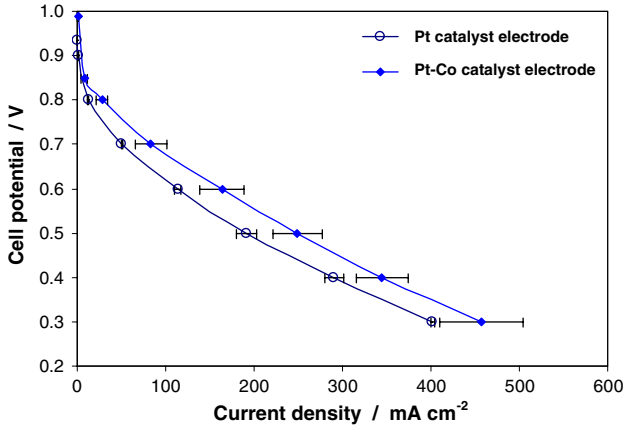

Fig. 4 Polarization curves of H_2/O_2 PEMFC with the Pt and Pt–Co catalyst electrodes prepared by DC electrodeposition at 2 C cm^{-2} and 10 mA cm^{-2}

the Pt structure to form an alloy. The Pt–Co composition mapping obtained by EDX analysis (not shown here) reveals that both Pt and Co distribute uniformly throughout the electrode surface.

The effect of alloying Pt with Co on catalyst activity and on catalyst properties, including alloy composition, lattice parameter, atomic distance and particle size, can be seen in Fig. 4 and Table 2, respectively. Figure 4 shows that the Pt–Co alloy catalyst electrode has better performance than the Pt catalyst electrode obtained under the same electrodeposition conditions. The polarization curves are also used to calculate the mass activities (i.e., the rate of oxygen reduction is normalized to activity per mg of Pt loading) of both Pt–Co alloy catalyst and Pt catalyst at 0.8 and 0.6 V. The electrodeposited Pt–Co alloy catalyst shows an enhancement in mass activity over the electrodeposited Pt catalyst by factors of 2.02 and 1.27 at 0.8 and 0.6 V, respectively. The improvement in the performance of the Pt–Co catalyst electrode indicates the enhancement of the catalyst activity for the ORR due to the addition of Co into the Pt structure [10]. By alloying Pt with Co, the Pt–Pt bond distance becomes shorter (0.22399 nm) compared to that of pure Pt catalyst (0.22621 nm), as shown in Table 2. The shorter atomic distance results in the weaker adsorption bond between oxygen and Pt surface to form hydroxide compounds. Thus, the reduction reaction of oxygen to form the intermediate species can proceed easier on Pt–Co surface than on Pt surface.

Moreover, as shown in Table 2, alloying Pt with Co by electrodeposition can reduce the particle size of the electrodeposited catalyst. The reduction in particle size of the electrodeposited Pt–Co alloy catalyst from that of the electrodeposited Pt catalyst will further enhance the electrocatalystic activity of the Pt–Co alloy catalyst. It is worth noting that the previous studies had reported that the sizes of Pt–Co alloy particles were normally bigger than those of Pt particles [10, 14–16] since most of them underwent heat treatment at high temperature (>700 °C) during the alloying process. This high-temperature heat treatment can facilitate sintering and coalescence of the catalyst particles resulting in the growing of the alloy catalyst particles. This is considered a drawback since big particle sizes of the Pt–Co alloy catalyst may lead to the decrease in the mass activity, although the Pt–Co alloy catalyst has been proved to have higher electrocatalytic activity towards the ORR than pure Pt. Our DC electrodeposition results here show that the particle size of the electrodeposited Pt–Co alloy is smaller than that of the electrodeposited Pt. This is considered to be an advantage for the preparation of the Pt–Co alloy catalysts by electrodeposition.

3.2 Pt–Co catalyst electrodes prepared by pulse current (PC) electrodeposition

By applying the current in a pulse waveform pattern, higher current density can be applied compared to DC electrodeposition without exceeding the mass transfer limitation since metal ions consumed during the on-time are recovered during the off-time where no metal ions are consumed [34, 36, 37]. In addition, there are various operating parameters—pulse current density (i_P), on-time (T_{on}), off-time (T_{off}), duty cycle (ratio of on-time to the pulse cycle period; θ) and frequency—that can be manipulated to obtain desired deposit structure, particle size and alloy composition (for alloy electrodeposition) compared to one operating parameter (i.e., applied current density) in DC electrodeposition.

Table 2 Comparisons of Pt:Co composition, catalyst loading, lattice parameter, atomic distance, particle size and mass activity of the Pt catalyst electrode and Pt–Co catalyst electrode prepared by DC electrodeposition at the charge density of 2 C cm^{-2} and the current density of 10 mA cm^{-2}

Catalyst electrode	EDX				XRD			Mass activity (mA $mg\ Pt^{-1}$)	
	Pt:Co alloy composition/ atomic ratio	Pt ($mg\ cm^{-2}$)	Co ($mg\ cm^{-2}$)	Total ($mg\ cm^{-2}$)	Lattice parameter (nm)	Atomic distance (nm)	Particle size (nm)	At 0.8 V	At 0.6 V
Pt/C	100:0	0.5840	–	0.5840	0.3920	0.22621	26.40	21.3	194.8
Pt–Co/C	88:12	0.6633	0.0274	0.6907	0.3880	0.22399	12.23	43.0	246.7

To study the preparation of the Pt–Co catalyst electrodes by pulse current electrodeposition, a series of experiments were conducted to investigate the effect of pulse plating parameters on the catalyst morphology and composition and on the fuel cell performance. To make a comparison, the information obtained from the Pt–Co catalyst electrode prepared by DC electrodeposition is used in the study of pulse current electrodepostion. Henceforth, unless stated otherwise, the pulse current electrodeposition will be conduced at the fixed charge density of 2 C cm^{-2} and the time-average current density (i_{avg}) of 10 A cm^{-2} in the solution having the same composition as considered in the previous section. The pulse conditions and information of catalyst composition, catalyst loading, lattice parameter, atomic distance, and particle size of Pt–Co catalysts are summarized in Table 3. The polarization curves and SEM images of the Pt–Co catalysts prepared at those conditions are shown in Figs. 5 and 6, respectively. TEM images, shown in Fig. 7, indicate the effect of the plating mode on the Pt–Co particle size. TEM results also confirm that the particle sizes estimated from XRD analysis are close to those estimated from TEM (Table 3).

The polarization curves in Fig. 5 show that the Pt–Co catalyst electrodes prepared by pulse current electrodeposition exhibit better performance than that prepared by DC electrodeposition. The enhancement of performance of the Pt–Co catalyst electrodes prepared by pulse current electrodepositon should be the result from the decrease in the Pt–Co particle sizes and the improved deposit structures, as shown in SEM in Fig. 6 and TEM in Fig. 7, which are influenced from substantially higher applied current densities compared to the current density used in DC electrodeposition (i.e., $i_P > i_{avg}$). Moreover, the step change in electrode potential at the beginning of each pulse cycle results in the continuous formation of nuclei throughout the deposition process. Electrocrystallization mechanism, then, changes from an instantaneous nucleation mechanism in the case of DC electrodeposition to progressive nucleation in the case of pulse current

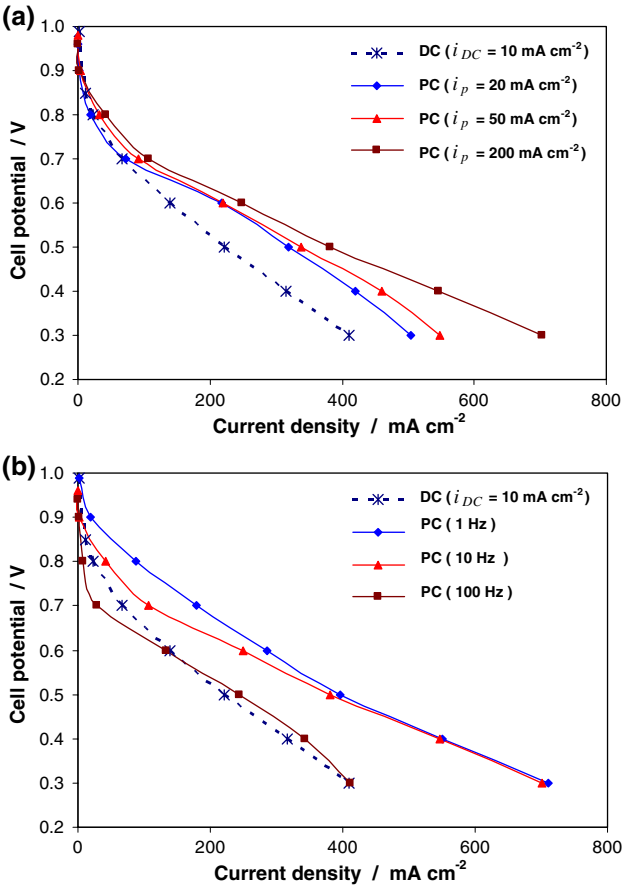

Fig. 5 Polarization curves of H_2/O_2 PEMFC with the Pt–Co catalyst electrodes prepared by pulse current electrodeposition using (**a**) 10 Hz and different pulse current densities; (**b**) 200 mA cm^{-2} and different frequencies

Table 3 Summary of pulse current electrodeposition conditions and Pt:Co composition, catalyst loading, lattice parameter, atomic distance, and particle size of the prepared Pt–Co catalysts

Pulse conditions			EDX				XRD		
Pulse frequency	i_p (mA cm^{-2})	Duty cycle (%)	Pt:Co alloy composition/atomic ratio	Pt (mg cm^{-2})	Co (mg cm^{-2})	Total (mg cm^{-2})	Lattice parameter (nm)	Atomic distance (nm)	Particle size (nm)
DC	10	–	88:12	0.6542	0.0270	0.6812	0.3880	0.22399	12.23[a]
1 Hz	200	5	88:12	0.4754	0.0196	0.4950	0.3882	0.22335	9.11
10 Hz	20	50	90:10	0.4828	0.0162	0.4990	0.3878	0.22378	12.22
	50	20	88:12	0.4889	0.0201	0.5090	0.3877	0.22376	10.82
	200	5	89:11	0.4704	0.0176	0.4880	0.3876	0.22350	8.95[b]
100 Hz	200	5	90:10	0.3986	0.0134	0.4120	0.3891	0.22398	10.24

[a] The particle size estimated from TEM image is found to be 14.21 nm (Fig. 7a)

[b] The particle size estimated from TEM image is found to be 7.45 nm (Fig. 7b)

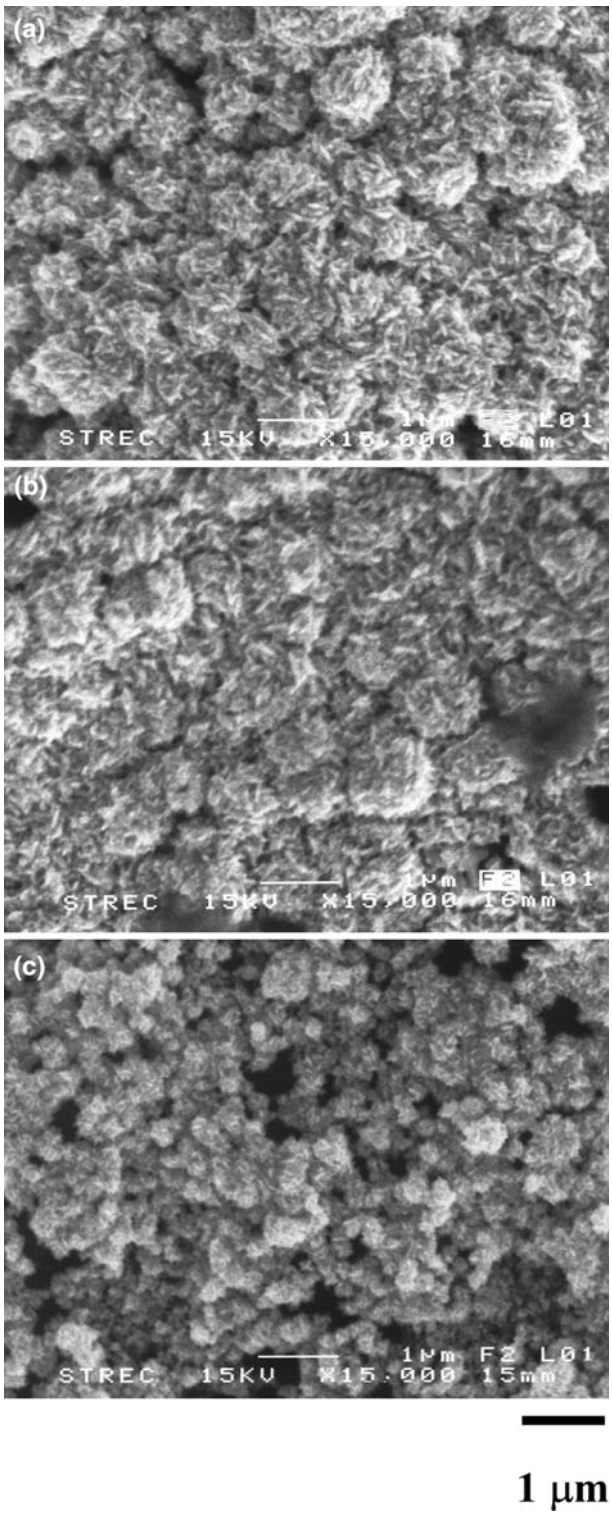

Fig. 6 SEM images of the Pt–Co catalyst electrodes prepared by pulse current electrodeposition at 10 Hz using pulse current densities of (**a**) 20 mA cm^{-2}; (**b**) 50 mA cm^{-2}; (**c**) 200 mA cm^{-2}

electrodeposition [38]. As a result, smaller-grained structure of the Pt–Co catalyst can be obtained by pulse current electrodeposition.

3.2.1 *Effect of pulse current density*

To investigate the effect of the applied pulse current density, we consider the experiments at the fixed pulse frequency of 10 Hz. For a fixed time-average current density, the pulse current density is varied depending on the duty cycle. Comparison of polarization curves in Fig. 5a shows that at the pulse frequency of 10 Hz the Pt–Co alloy catalysts produced at higher applied current densities tend to yield higher fuel cell performance, although the difference is not very significant at lower pulse current densities (i.e., 20 and 50 mA cm^{-2}). The noticeably higher performance is obtained from the Pt–Co alloy catalyst electrode prepared at the pulse current density of 200 mA cm^{-2}. The use of a greater pulse current density than 200 mA cm^{-2} (or lower duty cycle than 5%) is expected to push the electrodeposition process to take place closer to the mass transfer control conditions since the applied pulse current density can approach the pulse limiting current density [34]. Then, in this study, we limited the applied current density to 200 mA cm^{-2}. From SEM images shown in Fig. 6, it is clearly observed that the Pt–Co alloy catalyst produced at the pulse current density of 200 mA cm^{-2} consists of very small-grained particles (Fig. 6c and Table 3). Those small-grained particles combine to form fine-structured catalyst, while the Pt–Co alloy catalysts produced at lower pulse current densities (Fig. 6a, b) and by DC electrodeposition (Fig. 2b) appear to construct of big-grained particles with coarse structures. At significantly high applied current density (i.e., 200 mA cm^{-2}), electrode potential reaches the more negative value during each cathodic pulse so that the Pt–Co catalyst having smaller-grained particles and higher surface area are produced. As a result, the highest performance of the fuel cell is obtained.

3.2.2 *Effect of pulse frequency*

To study the effect of the pulse frequency, we consider the experiments conducted at the pulse current density of 200 mA cm^{-2}. The effect of the pulse frequency for Pt–Co electrodeposition on the fuel cell performance appears to be more pronounced than that of the pulse current density, as observed in Fig. 5b. The advantages of applying pulse current electrodeposition for catalyst preparation can be obviously seen in the Pt–Co catalysts prepared at lower pulse frequencies. The fuel cell performance of the electrode prepared at the lowest pulse frequency studied (i.e., 1 Hz) is the highest. When the pulse frequency used in the catalyst preparation is increased, the fuel cell performance deteriorates. The reason is that when the pulse frequency is increased, the electrical double layer effect becomes important and can affect the set pulse waveform [38, 39]. If

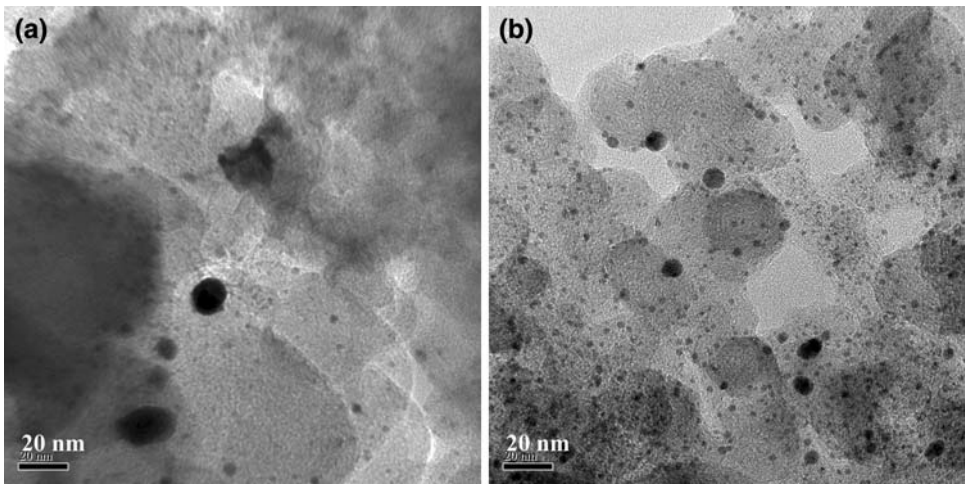

Fig. 7 TEM images of the Pt–Co catalyst electrodes prepared by (**a**) DC electrodeposition at 2 C cm^{-2} and 10 mA cm^{-2} and (**b**) pulse current electrodeposition using 200 mA cm^{-2} at 10 Hz

the pulse frequency is too high, the electrical double layer capacitance can alter the set pulse waveform to become a ripple DC signal. As a result, the electrodeposit obtained at very high pulse frequency can be similar to that obtained by DC electrodeposition [38]. This might explain the decrease in the fuel cell performance of the Pt–Co catalyst electrodes produced at higher pulse frequencies, as shown in Fig. 5b. Ultimately, the fuel cell performance of the Pt–Co catalyst electrode produced at 100 Hz decreases to the same level as that produced by DC electrodeposition.

It should be noted that the fuel cell performances of the Pt–Co catalyst electrodes obtained at various pulse conditions agree well with the characterization results of the corresponding Pt–Co catalyst electrodes. The Pt–Co catalysts obtained at higher pulse current densities or lower frequencies have shorter atomic distances, and smaller particles (Table 3) and yield higher performances (Fig. 5) than those obtained at lower pulse currents or higher frequencies. In addition, the EDX results reveal that neither pulse current densities nor pulse frequencies studied have the significant effect on the composition of Pt and Co deposited on the electrodes. Thus, the improvement in the performance of the Pt–Co catalyst electrodes by applying pulse current electrodeposition should be mainly due to the change in deposit structure rather than due to the composition of the Pt–Co catalysts which remains relatively unchanged.

3.2.3 *Effect of off-time*

In pulse current electrodeposition, besides the pulse current density and pulse frequency, the off-time is expected to play the major role. For pulse current electrodeposition of a single metal, the off-time is expected to influence the structure of the electrodeposit through the grain grow process of the existing crystals and through the mass transfer recovery process. For pulse current electrodeposition of a binary alloy, the effect of the off-time is expected to be more complicated. Besides the deposit structure, the off-time used can influence the electrodeposit composition since during the off-time the less noble metal can be selectively dissolved from the alloy by the more noble one through the displacement reaction. In this case, the duration of the off-time used can affect both the Pt–Co alloy catalyst structure and the Pt–Co composition.

The polarization curves of the Pt–Co catalyst electrodes prepared at different off-times are shown in Fig. 8. For each experiment the on-time, the pulse current density and the charge density are fixed at 0.05 s, 200 mA cm^{-2} and 2 C cm^{-2}, respectively. It, however, should be noted that by fixing the pulse current density and the on-time, while the off-time is varied, the time-average current density will be changed depending on the off-time used. From EDX analysis, the Pt:Co alloy compositions are still in the range of 90:10 where Pt:Co = 87:13 for T_{off} = 0.45 s and Pt:Co = 90:10 for T_{off} = 1.95 s. These results indicate that

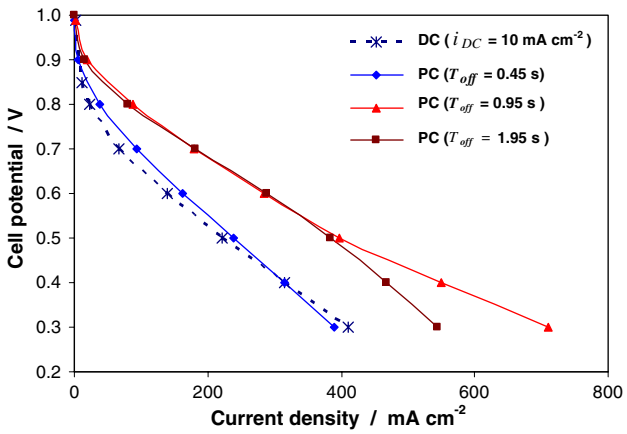

Fig. 8 Polarization curves of H_2/O_2 PEMFC with the electrodeposited Pt–Co catalyst electrodes prepared by pulse current electrodeposition using different off-times while the pulse current density, the charge current density and the on-time are fixed at 200 mA cm^{-2}, 2 C cm^{-2} and 0.05 s, respectively

although the displacement reaction between Pt and Co can take place during the off-time, the variation of the off-time does not affect the Pt and Co composition of the deposited Pt–Co catalysts in the conditions studied.

Figure 8 shows that the highest performance of the Pt–Co catalyst electrode is obtained when the off-time of 0.95 s is used for catalyst electrodeposition. The Pt–Co catalyst obtained at the shorter off-time leads to the significant depletion of the fuel cell performance compared to those obtained at the higher off-times which have relatively close activation polarizations. The decrease in the fuel cell performance when the off-time is lowered to 0.45 s and when the off-time is increased to 1.95 s should be due to the formation of bigger-grained structures as the results of the insufficient off-time for mass transfer recovery process and more extended period for the grain growth process, respectively.

3.2.4 *Effect of solution composition*

As observed above, the Pt and Co composition of the Pt–Co catalysts obtained under the conditions in this study is relatively unaffected by the deposition mode (i.e., DC or pulse current electrodeposition) and the pulse conditions. To study the influence of Pt and Co composition of the prepared catalysts on the fuel cell performance, several Pt–Co catalyst electrodes were prepared in different solution compositions, as listed in Table 4. All experiments are conducted at the pulse current density of 200 mA cm^{-2}, the time-average current density of 10 mA cm^{-2}, the pulse frequency of 1 Hz and the charge density of 2 C cm^{-2}. We tried to achieve the Pt–Co alloy catalysts having the Pt:Co compositions in the range between 90:10 and 10:90 by varying the composition of the deposition solution.

Table 4 shows that the Pt:Co alloy composition of the catalysts prepared is relatively independent on the concentration of Co in the deposition solution. When the concentration of Co in the solution is increased ten times from 0.1 to 1 M, the Pt:Co alloy composition of the catalyst is still relatively unchanged around the region of 88:10. On the other hand, the Pt:Co alloy composition of the prepared catalysts is varied depending on the Pt concentration in the deposition solution. By reducing the Pt concentration from 0.02 M to 0.015 M, 0.01 M, 0.005 M and 0.001 M, the Pt:Co alloy composition of the catalyst decreases from 88:10 to 82:18, 66:34, 21:79, and 10:90, respectively.

The SEM images of the Pt–Co alloy catalysts prepared in different solutions are presented in Fig. 9. They indicate that as the %Co content in the Pt–Co alloy catalysts increases, the particles of the catalysts tend to get smaller (Figs. 9a–d). The finer grained-structures of high %Co content are also confirmed by the XRD results shown in Table 4. However, if the %Pt content is too low (i.e., 21% Pt or lower in this study), the electrodeposited catalysts do not agglomerate to form grained-crystal structures, but instead form sponge-like amorphous structures, as shown in Fig. 9e, f. Formation of amorphous structures of low %Pt content alloy catalysts are observed through the change in XRD spectra as shown in Fig. 10. XRD spectra in Fig. 10 show that most peaks slightly shift to the higher 2θ values as the %Pt content in the Pt–Co catalyst decreases following the Vegard's law [40, 41]. In addition, when %Pt content in the Pt–Co catalyst decreases, the peaks of the spectra become shorter and broader, indicating the smaller particle sizes of the catalyst. When the Pt content reaches 20%, the (111) peak is very broad whereas other peaks almost disappear (Fig. 10e). Moreover, an additional peak is observed near the base of (111) peak, at $2\theta = 44.5°$, which should correspond to Co(111). The complete diminution of the previously existing peaks and a presence of a new flat-broad peak in the spectrum of the Pt–Co alloy catalyst having Pt:Co composition of 10:90 (Fig. 10f) indicate that Co becomes dominant in the Pt–Co

Table 4 Summary of Pt:Co composition, catalyst loading, lattice parameter, atomic distance and particle size of the Pt–Co catalysts prepared in different deposition solutions

Solution concentration (M)		EDX				XRD		
$H_2PtCl_6 \cdot 6H_2O$	$CoSO_4 \cdot 7H_2O$	Pt:Co alloy composition/ atomic ratio	Pt (mg cm^{-2})	Co (mg cm^{-2})	Total (mg cm^{-2})	Lattice parameter (nm)	Atomic distance (nm)	Particle size (nm)
0.02	0.1	88:12	0.4754	0.0196	0.495	0.3880	0.2234	9.11
0.02	1	86:14	0.4585	0.0225	0.481	0.3878	0.2206	8.87
0.015	0.1	82:18	0.4230	0.0280	0.451	0.3874	0.2198	8.47
0.01	0.1	66:34	0.3634	0.0566	0.420	0.3870	0.2121	7.72
0.005	0.1	21:79	0.2036	0.2314	0.435	0.3841	0.2101	12.56
0.001	0.1	10:90	0.1092	0.2968	0.406	0.3744	0.2081	17.47

All experiments were conducted at the pulse current density of 200 mA cm^{-2}, the time-average current density of 10 mA cm^{-2}, the pulse frequency of 1 Hz and the charge density of 2 C cm^{-2}

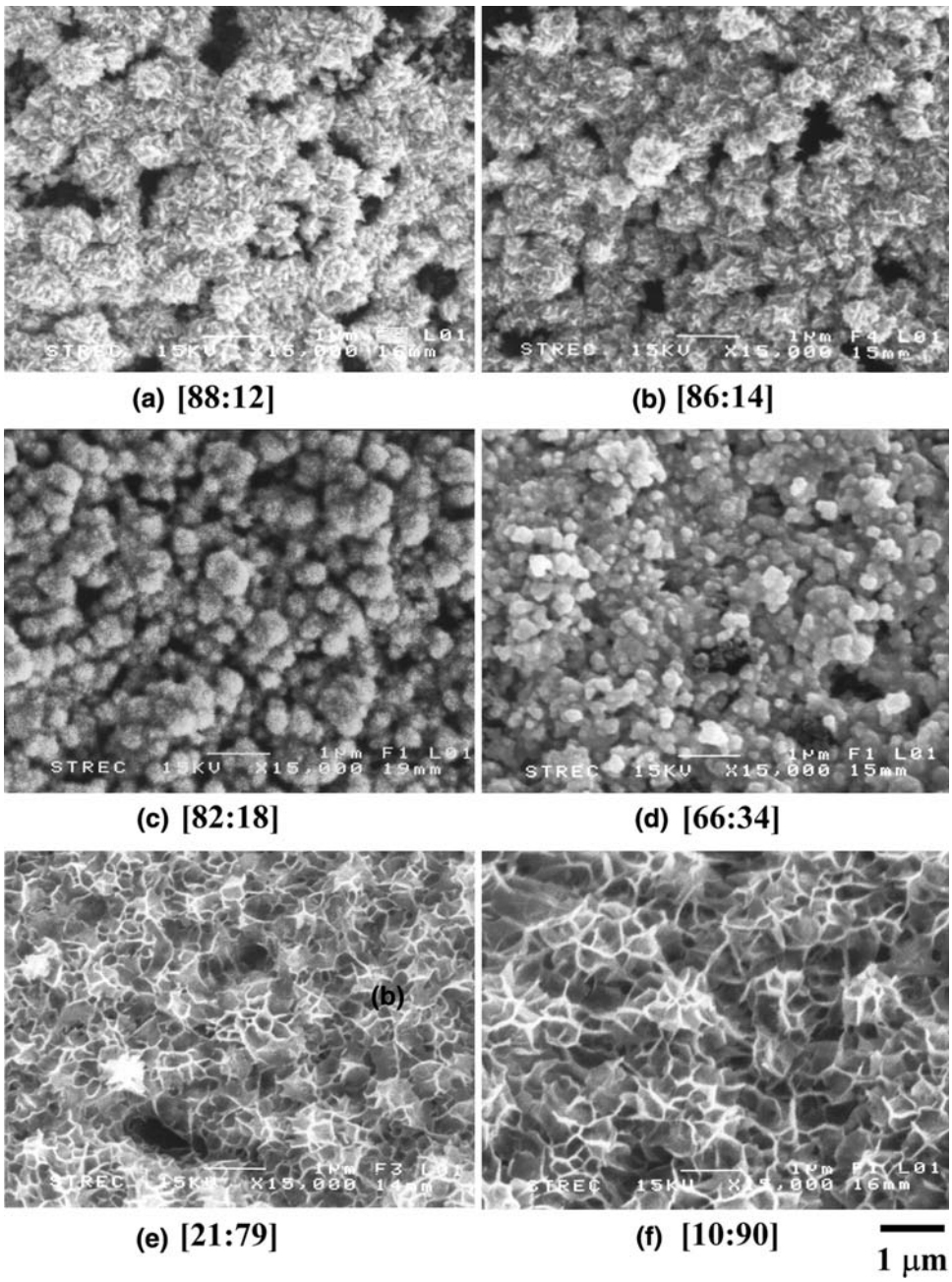

Fig. 9 SEM images of the Pt–Co catalyst electrodes prepared by pulse current electrodeposition using 200 mA cm^{-2} at 1 Hz in different deposition solutions. (**a**) 0.02 M $H_2PtCl_6 \cdot 6H_2O$ and 0.1 M $CoSO_4 \cdot 7H_2O$; (**b**) 0.02 M $H_2PtCl_6 \cdot 6H_2O$ and 1 M $CoSO_4 \cdot 7H_2O$; (**c**) 0.015 M $H_2PtCl_6 \cdot 6H_2O$ and 0.1 M $CoSO_4 \cdot 7H_2O$; (**d**) 0.01 M $H_2PtCl_6 \cdot 6H_2O$ and 0.1 M $CoSO_4 \cdot 7H_2O$; (**e**) 0.005 M $H_2PtCl_6 \cdot 6H_2O$ and 0.1 M $CoSO_4 \cdot 7H_2O$; (**f**) 0.001 M $H_2PtCl_6 \cdot 6H_2O$ and 0.1 M $CoSO_4 \cdot 7H_2O$. (The values shown in the square blankets indicate the Pt:Co ratios of the Pt–Co catalysts estimated from EDX)

alloy catalyst and the structure changes to amorphous form (Fig. 9f).

Figure 11 shows the polarization curves of the Pt–Co catalyst electrodes prepared in the different solution compositions. The ratio in each figure represents the Pt:Co composition of the Pt–Co catalyst. It shows that the Pt–Co catalyst having the Pt:Co content of 82:18 provides the highest fuel cell performance, although it does not have the highest amount of Pt in the catalyst. As discussed previously, alloying Pt with Co enhances the electroactivity from pure Pt catalyst. In addition, the Pt–Co catalysts with higher amounts of Co also have smaller particle sizes, as shown in SEM images (Fig. 9) and XRD results (Table 4). Then, the decrease in the particle size by increasing %Co content in the catalysts to the suitable amount can further improve the fuel cell performance due to the increase in active area of the catalyst. However, it is well-known that Pt is the best element for the ORR. If the amount of Pt present in the Pt–Co alloy catalyst is too low, the Pt–Co alloy catalyst will not be a good catalyst for the ORR. Then, the amounts of Pt and Co in the catalysts are needed to be optimized in order to balance the influences of Pt and Co on the electroactivity of the Pt–Co catalyst. Fig. 11 also indicates that although the Pt–Co alloy catalyst having

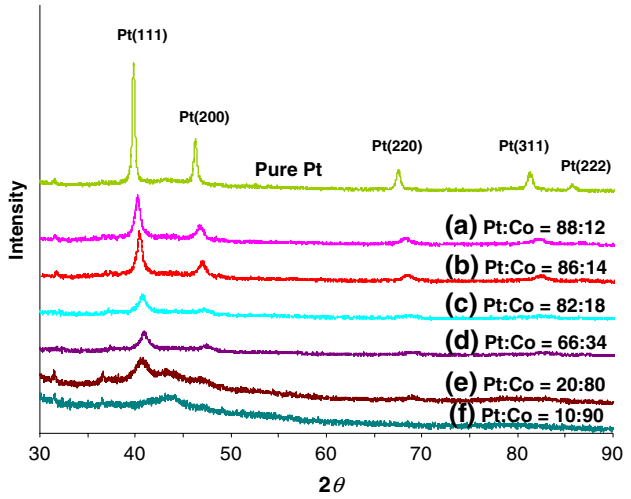

Fig. 10 X-ray diffraction patterns of the Pt–Co catalysts prepared by pulse current electrodeposition using 200 mA cm^{-2} at 1 Hz in different deposition solutions. The values shown in the figure represent the Pt:Co ratios of the Pt–Co catalysts corresponding to Fig. 9

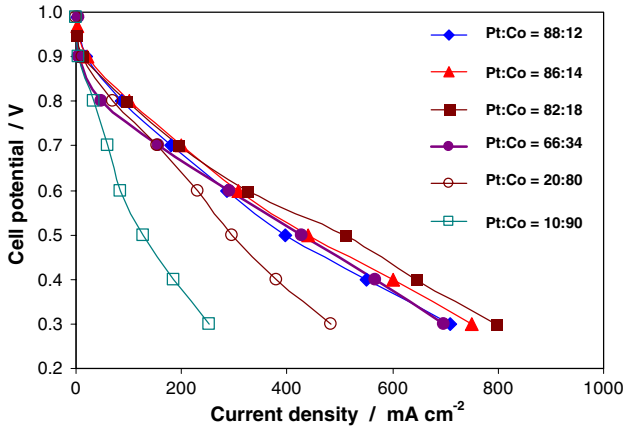

Fig. 11 Polarization curves of H_2/O_2 PEMFC with electrodeposited the Pt–Co catalyst electrodes prepared by pulse current electrodeposition using 200 mA cm^{-2} at 1 Hz in different deposition solutions. The values shown in the figure represent the Pt:Co ratios of the Pt–Co catalysts corresponding to Fig. 9

Pt:Co composition of 66:34 does not provide the highest fuel cell performance, it gives relatively similar fuel cell performance to several Pt–Co alloy catalysts having higher %Pt content. These results imply that the amount of Pt used for catalyzing the ORR in PEMFC can be substantially lowered from 0.584 mg cm^{-2} for pure Pt catalyst electrode to 0.277 mg cm^{-2} for the Pt–Co catalyst electrode having the Pt:Co composition of 66:34, while the fuel cell performance is higher.

It is worth noting that the particle sizes of the electrodeposited catalysts produced in this study are in the range of 7 nm which is considered relatively large compared to those reported by others (less than 5 nm). As mentioned earlier, the particle sizes of electrodeposited catalysts and three-phase contact are expected to be influenced by the properties of the pretreated electrode (i.e., non-catalyst electrode) [24, 27] such as the hydrophilic and hydrophobic properties. Thus, in order to obtain the desired particle sizes of the electrodeposited catalysts for the ORR, the preparation process of the non-catalyst electrodes is critical and shall be investigated more closely. Currently, our lab has been studying the preparation process of the non-catalyst electrodes to improve the surface properties which are suitable for catalyst preparation by electrodeposition. The optimized surface properties of non-catalyst electrodes are expected to provide the electrodeposited catalysts with smaller particle sizes, to improve three-phase contact and ultimately to enhance the electrocatalystic activity for the ORR.

4 Conclusions

Pt–Co alloy catalyst electrodes have been prepared by electrodeposition for the ORR in PEMFC. First, the preparation of Pt–Co alloy catalysts was conducted using DC electrodeposition where the suitable applied charge density and current density were found to be 2 C cm^{-2} and 10 mA cm^{-2}, respectively. DC results show the improvement in the electrocatalytic activity by alloying Pt with Co. By applying the current in the pulse waveform pattern, the applied pulse current density can be significantly high compared to the current density of DC electrodeposition without the violation of mass transfer limitation and thus the grain sizes of the Pt–Co alloy catalysts can be reduced. Of the conditions studied, pulse current electrodeposition using the pulse current density of 200 mA cm^{-2} at 1 Hz and 5% duty cycle was found to produce the best Pt–Co alloy catalyst which consists of the smallest-grained particles and was found to yield the highest fuel cell performance. However, neither the electrodeposition mode nor electrodeposition parameters have shown to have the substantial influence on the Pt–Co alloy catalyst composition. To vary the Pt–Co alloy composition, the amount of Pt present in the electrodeposition solution was found to be the significant factor. The Pt–Co alloy catalyst having the Pt:Co alloy composition of 82:18 was found to provide the highest fuel cell performance among the compositions studied. This study shows the promising results of developing the electrocatalyst and developing the electrode preparation process for the ORR used in PEMFC since the electroactivity of the catalyst is enhanced while the amount of Pt loading is reduced by alloying Pt with cheap Co metal using electrodeposition.

Acknowledgement The authors express their gratitude to National Center of Excellence for Petroleum, Petrochemicals and Advanced Materials for financial support during the course of this study.

References

1. Larminie J, Dicks A (2003) Fuel cell systems explained, 2nd edn. John Wiley & Sons, Chichester, England
2. Mukerjee S, Srinivasan S (1993) J Electroanal Chem 357:201
3. Toda T, Igarashi H, Uchida H, Watanabe M (1999) J Electrochem Soc 146:3750
4. Toda T, Igarashi H, Watanabe M (1999) J Electroanal Chem 460:258
5. Min M, Cho J, Cho K, Kim H (2000) Electrochim Acta 45:4211
6. Paulus UA, Wokaun A, Scherer GG, Schmidt TJ, Stamenkovic V, Markovic NM, Ross PN (2002) Electrochim Acta 47:3787
7. Shukla K, Neergat M, Bera P, Jayaram V, Hegde MS (2001) J Electroanal Chem 504:111
8. Xiong L, Kannan AM, Manthiram A (2002) Electrochem Commun 4:898
9. Stamenkovic V, Schmidt TJ, Ross PN, Markovic NM (2003) J Electroanal Chem 554:191
10. Xiong L, Manthiram A (2005) Electrochim Acta 50:2323
11. Antolini E, Salgado JRC, Gonzalez ER (2005) J Electroanal Chem 580:145
12. Paulus UA, Wokaun A, Scherer GG, Schmidt TJ, Stamenkovic V, Radmilovic V, Markovic NM, Ross PN (2002) J Phys Chem 106:4181
13. Salgado JRC, Antolini E, Gonzalez ER (2004) J Power Sources 138:56
14. Antolini E, Salgado JRC, Giz MJ, Gonzalez ER (2005) Int J Hydrogen Energy 30:1213
15. Huang Q, Yang H, Tang Y, Lu T, Akins DL (2006) Electrochem Commun 8:1220
16. Lu Y, Reddy RG (2007) Electrochim Acta 52:2562
17. Lopes T, Antolini E, Colmati F, Gonzalez ER (2007) J Power Sources 164:111
18. Neergat M, Shukla AK, Gandhi KS (2001) J Appl Electrochem 31:373
19. Travitsky N, Ripenbein T, Golodnitsky D, Rosenberg Y, Burshtein L, Peled E (2006) J Power Sources 161:782
20. Yu P, Pemberton M, Plasse P (2005) J Power Sources 144:11
21. Martz N, Roth C, Furß H (2005) J Appl Electrochem 35:85
22. Paunovic M, Schlesinger M (1998) Fundamentals of electrochemical deposition. Wiley, New York
23. Kim H, Subramanian NP, Popov BN (2004) J Power Sources 138:14
24. Duarte MME, Pilla AS, Sieben JM, Mayer CE (2006) Electrochem Commun 8:159
25. Thompson SD, Jordan LR, Forsyth M (2001) Electrochim Acta 46:1657
26. Choi KW, Kim HS, Lee TH (1998) J Power Sources 75:230
27. Kim H, Popov BN (2004) Electrochem Solid St 7:A71
28. Warren BE (1969) X-ray diffusion. Addison-Wesley, Reading, MA
29. Baumgartner ME, Raub CJ (1988) Plat Met Rev 32:188
30. Rao CRK, Trivedi DC (2005) Coord Chem Rev 249:613
31. Liu Y, Pritzker M (2003) J Appl Electrochem 33:1143
32. Amstrong MJ, Muller RH (1991) J Electrochem Soc 138:2303
33. Budevski E, Staikov G, Lorenz WJ (1996) Electrochemical Phase formation and growth. VCH, New York
34. Chène O, Landolt D (1989) J Appl Electrochem 19:188
35. Zhang X, Chan KY (2002) J Mater Chem 12:1203
36. Ibl N, Puippe JC, Angerer H (1978) Surf Tech 6:287
37. Puippe JC, Ibl N (1980) Plat Surf Finish 6:68
38. Tantavichet N, Pritzker MD (2005) Electrochim Acta 50:1849
39. Tantavichet N, Pritzker MD (2003) J Electrochem Soc 150:C665
40. Watanabe M, Uchida M, Motoo S (1987) J Electroanal Chem 229:395
41. Park J, Cheon J (2001) J Am Chem Soc 123:5743